JOURNAL OF PROPULSION AND POWER
Vol. 18, No. 2, March–April 2002

Design Analysis of a Satellite Hydrazine Propulsion System

An-Shik Yang*
Da Yeh University, Chang Hwa 51505 Taiwan, Republic of China
and
Tien-Chuan Kuo†
National Space Program Office, Hsin Chu 30077 Taiwan, Republic of China

Numerical simulations are conducted to study various features of the key design parameters for a hydrazine-based satellite propulsion system. For the steady-state fluid analysis, a flow-channel network numerical scheme is used to determine the blowdown profile and the pressure drops in the propellant line, as well as the blowdown characteristics during the operation lifetime of the propulsion system. For the transient fluid analysis, a theoretical model based on the method of characteristics is solved to simulate the time-dependent transport behavior of the propellant flows. The pressure responses at the inlets of the latch isolation valve and thruster valves for the conditions of different thrust force levels, different equipping orifices, different pipeline lengths, and different open/closed periods in 0.25-s control cycle were studied. Predicted results indicate that better blowdown behaviors can be obtained for a satellite employing a bigger tank because the fixed propellant mass was loaded to the propulsion system. Better performances can also be achieved for smaller thrust level thrusters used on the satellite. When an appropriate orifice is equipped into the pipeline, the pressure fluctuation can be damped out rapidly and the potential risk of damaging the propulsion components is minimized. An optimum thruster valve opening time of 80 ms for the pulse-mode control is also recommended.

Nomenclature

A = pipe cross-sectional area
A_p = wetted peripheral area
a = acoustic speed
C = pipe anchored function
D = pipe diameter
E = Young's modulus
e = pipe thickness
F = thrust
f = friction factor
g = acceleration of gravity
I_{sp} = specific impulse
K = bulk modules of fluid
K_f = loss coefficient of filter
K_{lv} = loss coefficient of latching valve
K_{or} = loss coefficient of orifice
k = loss coefficient
L = pipe length
$\dot{m}$ = mass flow rate
P = pressure
P_t = tank pressure
P_u = thruster inlet pressure
P_0 = reference pressure
R = gas constant
T = temperature
t = time
u = local mean velocity
V = pressurant volume
v = velocity
W = weighting function
α = tilt angle of the pipe
ΔP_f = pressure drop of filter
ΔP_{lv} = pressure drop of latching valve
ΔP_p = pressure drop of lines
θ = gradient of the pipe wall
ρ = density
ρ_0 = reference density
σ = area change rate
τ = dimensionless time, identical to vt/D^2
τ_w = wall shear stress

Received 18 February 2001; revision received 22 June 2001; accepted for publication 1 December 2001.

*Assistant Professor, Department of Mechanical Engineering; asyang@mail.dyu.edu.tw. Senior Member AIAA.
†Associate Researcher, Mechanical Engineering Section; tckuo@nspo.gov.tw. Member AIAA.

Introduction

HYDRAZINE propulsion systems are a widely used type of propulsion to provide the required impulse for satellite orbit transfer and attitude control due to their advantages of low cost, technical simplicity, high reliability, and relative stability under normal storage.[1] A hydrazine propulsion system consists of hydrazine thrusters to produce thrust, a propellant tank to store propellant, and various components and assemblies (such as latching isolation valves, pressure transducer, filter, fill/drain valves, and plumbing) associated with conditioning, controlling, and transferring propellant. It is furnished as a module that is readily integrated into a satellite to a broad range of requirements with lightweight construction.[2–4]

A hydrazine propulsion system normally functions in a blowdown manner. A propellant/pressurant tank with a built in propellant management device (PMD) is used to ensure a steady supply of gas-free propellant under all satellite orientations. The high-pressure pressurant gas (nitrogen or helium) provides a pressure force to drive the liquid propellant (hydrazine) flowing from the tank to the thrusters. As the liquid propellant is expelled from the tank, the pressurant pressure drops throughout the lifetime of propellant usage. A blowdown hydrazine propulsion system operates in either continuous or pulse mode. In continuous mode operation, thrusters burn for an extended time period, depending on different thruster characteristics. Because the propulsion performance parameters (such as thrust and specific impulse) are strongly affected by the system pressure, the determination of the blowdown pressure profile for the whole lifetime period during propellant usage is one of major concerns in propulsion system design.

Table 1 Pipeline[a] length and tube bend data for ROCSAT-1 Propulsion System

No.	From	To	Length, mm	Number of bending angles				
				22.5 deg	67.5 deg	90.0 deg	135.0 deg	157.5 deg
1	Tank	Filter	845	3	0	4	0	0
2	Filter	Orifice	203	0	0	1	0	1
3	Orifice	ISO[b] valve	237	0	0	1	0	0
4	ISO valve	TJ[c] #1	647	3	2	0	1	0
5	TJ #1	TJ #2	47	0	0	0	0	0
6	TJ #1	TJ #3	468	3	0	0	0	0
7	TJ #2	DTM[d] #1	700	3	0	2	0	0
8	TJ #2	DTM #4	1122	6	0	3	0	0
9	TJ #3	DTM #2	700	3	0	2	0	0
10	TJ #3	DTM #3	1113	6	0	3	0	0

[a]Outer diameter and the wall thickness of the pipeline are 6.35 mm (0.25 in.) and 0.4064 mm (0.016 in.), respectively.
[b]Isolation valve.
[c]Tee junction.
[d]Dual thruster module.

In pulse-mode operation, thrusters are successively fired on–off to produce a series of impulse bits. Various approaches have been proposed for satellite attitude control with pulse-mode thruster firing. Pulse modulators, the most common approach, generate a pulse command sequence to the thruster valves by adjusting pulse width and/or pulse frequency, which can provide the benefits of better propellant economy, smoother control action, and closer to linear actuation.[5–7] The shut-off motion of the thruster valve can simultaneously introduce fluid-hammer (equivalent to water-hammer) pressure spikes in the pipe. For this kind of operation, the magnitude of the fluid-hammer pressure spikes must be considered in a propulsion design to assure system integrity.[8,9] When the transport behavior of a transient pulsating pipe flow is probed, the conventional steady-state Darcy friction formula may cause a significant error in simulating the strong damping of flow and pressure waves traveling through fluid lines. Zielke[10] developed a modified method of characteristics (MOC) including the effect of a frequency-dependence friction term. The calculated results demonstrated accurate predictions of the response pressure fluctuations due to an instantaneous valve closure. Trikha[11] improved the Zielke's model[10] to enhance its computational efficiency substantially. Schohl[12] further employed the least-square-fitting method to extend its applicable range with better prediction accuracy.

In the past, most of research related to monopropellant propulsion systems has been focused on the propulsion characteristics of thrusters. Limited studies have addressed the steady-state and transient flow phenomena of a hydrazine propulsion system. The pressurant and propellant flow in a hydrazine propulsion system can be numerically simulated to describe a flow and pressure balance in the propellant path through the system. This type of analysis can generally characterize the propellant mass flow rate and component/line pressure loss with respect to the tank pressure, as well as the propellant flow transient properties, which are very crucial for propulsion module design.

In the present work, the design configuration of the first satellite of Taiwan, Republic of China (ROCSAT-1) hydrazine propulsion system is adopted as an illustrative case for study. ROCSAT-1, launched 27 January 1999, is a low-Earth orbit science experimental satellite. The satellite circles the Earth at an altitude of 600 km with an inclination angle of 35 deg. The scientific experiments conducted for ROCSAT-1 include ocean color imaging, experiments on ionospheric plasma and electrodynamics, and experiments using Ka-band communication payloads.[13] The onboard hydrazine propulsion system is mainly used for orbit corrections at the final operational orbit and for attitude control during orbit insertion and contingency modes of operation. The objective of this paper is to perform a design analysis for hydrazine propulsion systems, specifically studying the effects of various design variables (such as tank volume, propellant mass flow rate based on the corresponding thrust force level, flow resistance of components, and duration setting of pulse trains) on the propulsion system performance.

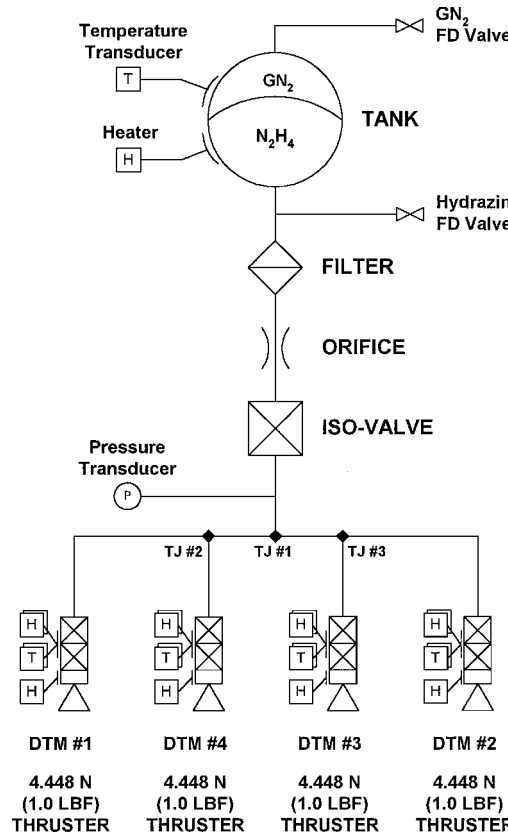

Fig. 1 Schematic of ROCSAT-1 propulsion subsystem.

Theoretical Formulation

A schematic diagram and the pipeline data of the ROCSAT-1 hydrazine propulsion system are shown in Fig. 1 and Table 1, respectively. The system is an all-welded blowdown-based hydrazine propulsion module. A spherical titanium propellant tank with an elastomeric diaphragm is used to provide gas-free propellant delivery for all satellite orientations. Inside a thruster, impulse is produced through the catalytic decomposition of monopropellant grade hydrazine.

Steady-State Modeling

The present mathematical model considers the ROCSAT-1 monopropellant feed system with various inline components including a propellant tank, a filter, an orifice, a latching isolation valve, and four thrusters. The pressurant (nitrogen) is used to pressurize the hydrazine propellant. To simulate the blowdown behavior of a

single-phase liquid propellant feed system, the conservation equations of mass and momentum are formulated and solved numerically using the flow-channel network numerical method. The volume of pressurant is first estimated based on an initially guessed value of propellant mass flow rate. The pressurant pressure is then calculated by the ideal-gas equation. As the propellant flows through the pipelines and components, the pressure drops along the pipelines and across each component at a certain mass flow rate, which is computed employing the associated friction correlations. With the momentum equation, the thruster inlet pressure is readily obtained and in turn can be applied to determine the propellant mass flow rate, thrust force, and specific impulse from the known characteristics of the thruster. Because the pressure drops are strongly coupled with the propellant mass flow rate, an iteration procedure is required to achieve a converged solution.

The governing equations used in the steady-state modeling are given as next.

Tank region:

$$V(t) = V_0 + \int_0^t \frac{\dot{m}_{\text{prop}}}{\rho}\,\mathrm{d}t \tag{1}$$

$$T(t) = T_0 \tag{2}$$

$$P(t) = nRT(t)/V(t) \tag{3}$$

where V_0 is the initial volume of the pressurant.

Pressure drop along the propellant lines:

$$P_t - P_u = \Delta P_p + \Delta P_f + \Delta P_{\text{or}} + \Delta P_{\text{lv}} \tag{4}$$

Line pressure drop:

$$\Delta P_p = \frac{\rho v^2}{2}\left(\frac{fL}{D} + \sum k\right) \tag{5}$$

where $f = 64/Re_D$. The term Σk stands for the sum of friction loss coefficients including theoretical estimates for tees, miter bends, and elbows.

Filter pressure drop:

$$\Delta P_f = (\rho v^2/2)K_f \tag{6}$$

Orifice pressure drop:

$$\Delta P_{\text{or}} = (\rho v^2/2)K_{\text{or}} \tag{7}$$

Latching valve pressure drop:

$$\Delta P_{\text{lv}} = (\rho v^2/2)K_{\text{lv}} \tag{8}$$

where K_f, K_{or}, and K_{lv} are functions of propellant mass flow rate and are obtained from component-level experimental correlation data. Based on component test data reports, the K factors of the propulsion components can be reasonably treated as a constant for the flow rate range in the present study.

Thruster Characteristics

From the hot-firing test data, the thruster characteristics including the propellant mass flow rate, the thrust, and the specific impulse can be correlated with the inlet pressure of the thruster, namely,

$$\dot{m}_{\text{prop}} = f[P_u], \qquad F = g[P_u], \qquad I_{\text{sp}} = h[P_u] \tag{9}$$

Transient Modeling

The time-dependent transport behavior modeling of the propellant in the ROCSAT-1 hydrazine propulsion system is studied. The governing equations used in the present study are given as follows. A more detailed formulation may be found in Ref. 14.

Continuity equation:

$$\frac{1}{\rho a^2}\frac{\mathrm{D}P}{\mathrm{D}t} + \frac{\partial u}{\partial x} + \frac{u\sigma}{A} = 0 \tag{10}$$

where σ is the change rate of the cross-sectional area along the x direction, that is, $\sigma(x) = \partial A/\partial x$. The acoustic speed can be determined by

$$a = \left[\frac{K/\rho}{1 + C(KD)/Ee}\right]^{\frac{1}{2}} \tag{11}$$

C is a function of Poisson's ratio whose form depends on the pipe restraint conditions.

Momentum equation:

$$\rho\frac{\partial u}{\partial t} + \rho u\frac{\partial u}{\partial x} = -\frac{\partial P}{\partial x} - \rho g\sin\alpha - \frac{\tau_w A_p \cos\theta}{A\,\mathrm{d}x} \tag{12}$$

The fluid is considered to be slightly compressible with high bulk modules, and the relationship between the fluid density and the pressure is given by

$$\frac{\mathrm{d}P}{\mathrm{d}\rho} = \frac{K}{\rho} \qquad \text{or} \qquad P = P_0 + K\,\ell n\frac{\rho}{\rho_0} \tag{13}$$

The equations of the conservation of mass and momentum establish a set of hyperbolic-type partial differential equations, and MOC can be applied to analyze this fluid transient problem. When Eqs. (9) and (11) are transformed by the MOC, the velocity, pressure, density, and acoustic speed in terms of x and t can be solved by the following sets of ordinary differential equations:

$$C^+: \begin{cases} \dfrac{\mathrm{d}x}{\mathrm{d}t} = u + a \\ \dfrac{1}{\rho a}\dfrac{\mathrm{d}P}{\mathrm{d}t} + \dfrac{\mathrm{d}u}{\mathrm{d}t} + g\sin\alpha + \dfrac{A_p\tau_w\cos\theta}{A\rho\,\mathrm{d}x} + \dfrac{ua}{A}\sigma(x) = 0 \end{cases} \tag{14}$$

$$C^-: \begin{cases} \dfrac{\mathrm{d}x}{\mathrm{d}t} = u - a \\ \dfrac{1}{\rho a}\dfrac{\mathrm{d}P}{\mathrm{d}t} - \dfrac{\mathrm{d}u}{\mathrm{d}t} - g\sin\alpha - \dfrac{A_p\tau_w\cos\theta}{A\rho\,\mathrm{d}x} + \dfrac{ua}{A}\sigma(x) = 0 \end{cases} \tag{15}$$

In modeling the frequency-dependent frictional losses of the unsteady laminar pipe flow, the wall shear stress τ_w can be related to the instantaneous mean velocity and the weighted past velocity change. This weighting function is basically a function of the dimensionless time τ, which is defined as $\tau = (\nu/D^2)t$. Schohl[12] used the least-square-fitting method for processing 143 exact data points and recommended a five-term approximate function to treat the dimensionless time as small as 10^{-5}. In the present work, the following eight-term approximate function is proposed to employ a nonlinear least-square approach for achieving a higher prediction accuracy with the dimensionless time resolution down to 10^{-7} and to increase the computation efficiency by avoiding massive storage of the entire flow history while computing the weighted past velocity change:

$$\begin{aligned} W(\tau) = {} & 1.0e^{-26\tau} + 2.3e^{-100\tau} + 9.1e^{-670\tau} \\ & + 29.5e^{-6{,}500\tau} + 75e^{-57{,}990\tau} + 205e^{-407{,}700\tau} \\ & + 445e^{-2{,}657{,}000\,\tau} + 875e^{-13{,}260{,}000\tau} \end{aligned} \tag{16}$$

The initial condition of the simulation is obtained by solving the following equations:

$$\frac{1}{\rho a^2}\frac{\mathrm{d}P}{\mathrm{d}x} + \frac{1}{A}\sigma(x) + \frac{1}{u}\frac{\mathrm{d}u}{\mathrm{d}x} = 0$$

$$\frac{\mathrm{d}P}{\mathrm{d}x} + \rho u\frac{\mathrm{d}u}{\mathrm{d}x} + \rho g\sin\alpha + \frac{A_p\tau_w\cos\theta}{A\,\mathrm{d}x} = 0 \qquad (17)$$

The pressure at the tank outlet is set to be a constant value of 24.5 bar, and the thruster inlet velocity at $t = 0^+$ is 0 m/s due to the sudden closure of the valve.

Results and Discussion

An experimental propellant feed system was established to conduct the blowdown experiment for measuring a continuous pressure drop of the pressurant as the propellant was discharged continuously. The experimental data were obtained to validate the present steady-state computer program. Comparisons of the results have demonstrated excellent agreement between the calculated and measured pressure–time histories at the locations of the propellant tank and the thruster inlet. More detailed information may be found in Ref. 15. For the time-dependent flow study, the transient flow formulation, together with the MOC, was verified by comparing with Simpson's experimental data.[16] A long straight pipe was set up horizontally with the mounting of an upstream constant-pressure tank and a downstream fast-closing ball valve. The pressure waves were generated due to the closing of the downstream ball valve (with the valve closure time of 0.015 s). The predictions were found to agree well with the pressure-wave measurements.

Numerical simulations were conducted for the following baseline condition. The total internal volume of the propellant tank is 0.091 m^3, with a qualified propellant storage capacity of 72.6 kg. Nitrogen is used to pressurize the hydrazine propellant with the initial pressure of 24.5 bar. All lines from the tank outlet to the inlet of thruster valves are first filled with hydrazine. Because the propellant tank is externally covered by multilayer insulation with heaters attached for the temperature control, the temperatures of pressurant and propellant are nearly same and can reasonably stay quite constant during the mission. In computation, the temperature of nitrogen and hydrazine is set to be T_0 with a nominal value of 15.6°C, which is an orbital average temperature for imitating inorbit situations. The influence of expansion and heat transfer on the variation of gas temperature is ignored.

In this analysis, four thrusters are considered to be firing simultaneously in the steady-state operation mode over the blowdown pressure range. The effects of tank expansion, hydrazine vapor pressure, and solubility are neglected. The friction coefficients K_f, K_{or}, and K_{lv} [shown in Eqs. (6), (7), and (8)] are computed by linear approximation of the working points given in the component equipment specifications. These working points of the pressure drop/mass flow rate relationship for each propulsion component are listed as follows: 1) filter, 7560.0 Pa at 7.576 g/s; 2) orifice, 51,900.0 Pa at 7.576 g/s; and 3) latching valve, 16400.0 Pa at 7.576 g/s. From the hot-firing acceptance test data at the vacuum condition for the thrusters used in the ROCSAT-1 program, the propellant mass flow rate passing through a 4.448-N (1-lbf) thruster is correlated to the thruster inlet pressure as $\dot{m}_{\mathrm{prop}} = (2.222 \times 10^{-5}) \times P^{0.774}$, where the units of $\dot{m}_{\mathrm{prop}}$ and P are gram per second and pascal, respectively.

To design a satellite hydrazine propulsion system, the tradeoffs of various design features must be conducted based on mission requirements. The system will be then sized iteratively until the best configuration is attained. During the sizing process, the qualified capability ranges of key design parameters are examined in detail to properly configure tanks, thrusters, and flow components to be implemented in the propulsion system. The tank sizing process is first performed for the ROCSAT-1 hydrazine propulsion system. In this work, three potential tanks were considered with the tank volume of 91, 96, and 104 liter, respectively. Main characteristics of those tanks are given in Table 2. Figure 2 shows the tank pressure profiles with respect to the remaining propellant mass for three different tanks. In the calculations, three blowdown curves are based on the same initial tank pressure of 24.5 bar with the identical propellant loading onboard of 72.6 kg for all proposed tanks. Corresponding to the remaining hydrazine mass from 72.6 kg to null, the three predicted blowdown pressure profiles range from 24.5 bar at beginning of life (BOL) to 4.96, 5.98, and 7.40 bar at end of life (EOL) for the internal tank volume of 91, 96, and 104 liter. For all three cases, the tank pressure in the early phase of the event reduces at a relatively faster rate than that at the later phase of the event. This is because the pressurant occupies a lower percentage of the internal volume of the tank in the beginning, whereas a greater pressure decrease can be introduced subsequently by the free volume produced through the propellant consumption in the tank. Compared with the pressure profile for a larger tank, the pressure for a smaller tank tends to drop relatively faster in the primitive development stage of the blowdown phenomenon. Therefore, for any fixed value of remaining hydrazine mass (Fig. 2), it is clearly observed that the pressure for a bigger tank, for example, the 104-liter tank, is constantly greater than that for a smaller tank (the 91-liter tank).

Table 2 Main characteristics of potential tanks considered in tank sizing process

Supplier	PSI	DOWTY	DASA
Type	Diaphragm	Diaphragm	Surface tension
Shape	Spherical	Spherical	Spherical
Mass, kg	6.7	8.2	6.4
Volume, liter	91	96	104
Qualified propellant capacity, kg	72.6	74.5	81

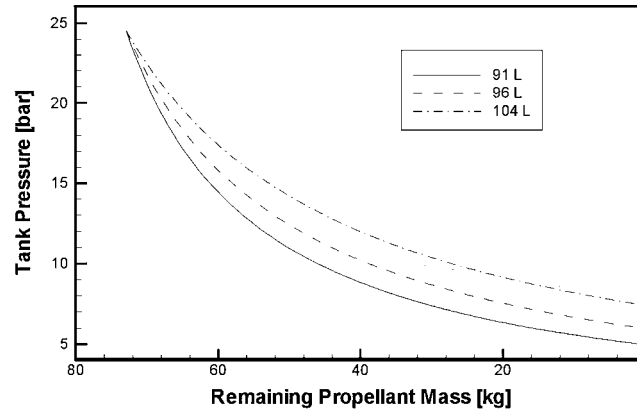

Fig. 2 Blowdown pressure profiles for three different tanks.

Figure 3 shows the steady-state mass flow rate and component/line pressure losses vs the tank pressure for three different tank sizes. For the same initial tank pressure of 24.5 bar, the total mass flow rate and total line loss from tank to thruster (defined by the sum of pressure losses for all components and line) are 7.80 g/s and 1.03 bar, respectively. At EOL, both hydrazine mass flow rate and total line loss for a larger tank are higher than those for a smaller tank. In general, the pressure loss in the lines is small because the inline propellant mass flow rate is quite low for the corresponding thrust force from 1 to 8.896 N. Furthermore, the thruster inlet pressure can be deduced by subtracting the total line loss from the known tank pressure and plugged into Eq. (9) for determining the propulsive performance characteristics including the thrust and the specific impulse I_{sp}, as shown in Fig. 4. Over the blowdown pressure range, predicted values of thrust/I_{sp} for the tank volume of 91, 96, and 104 liter are 1.38–4.35 N/203–224 s, 1.58–4.35 N/206–224 s, and 1.84–4.35 N/209–224 s, respectively. The design performance of the hydrazine propulsion system using the 104-liter tank shows an enhancement over the system employing the 91-liter tank. Notably, a 33% thrust force increase and a 3% specific impulse improvement can be achieved as the tank pressure reaches the point of EOL.

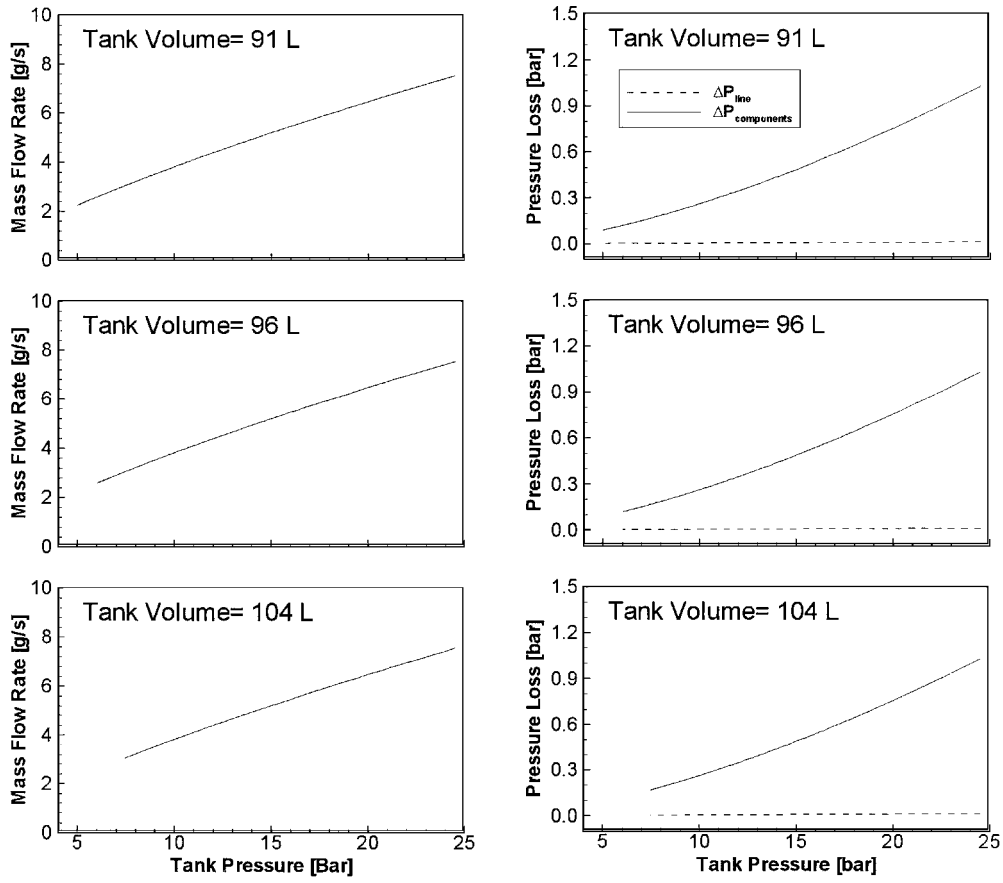

Propellant mass flow rate **Component/line pressure drop profiles**

Fig. 3 Steady-state mass flow rate and component/line pressure losses vs tank pressure for three different tanks.

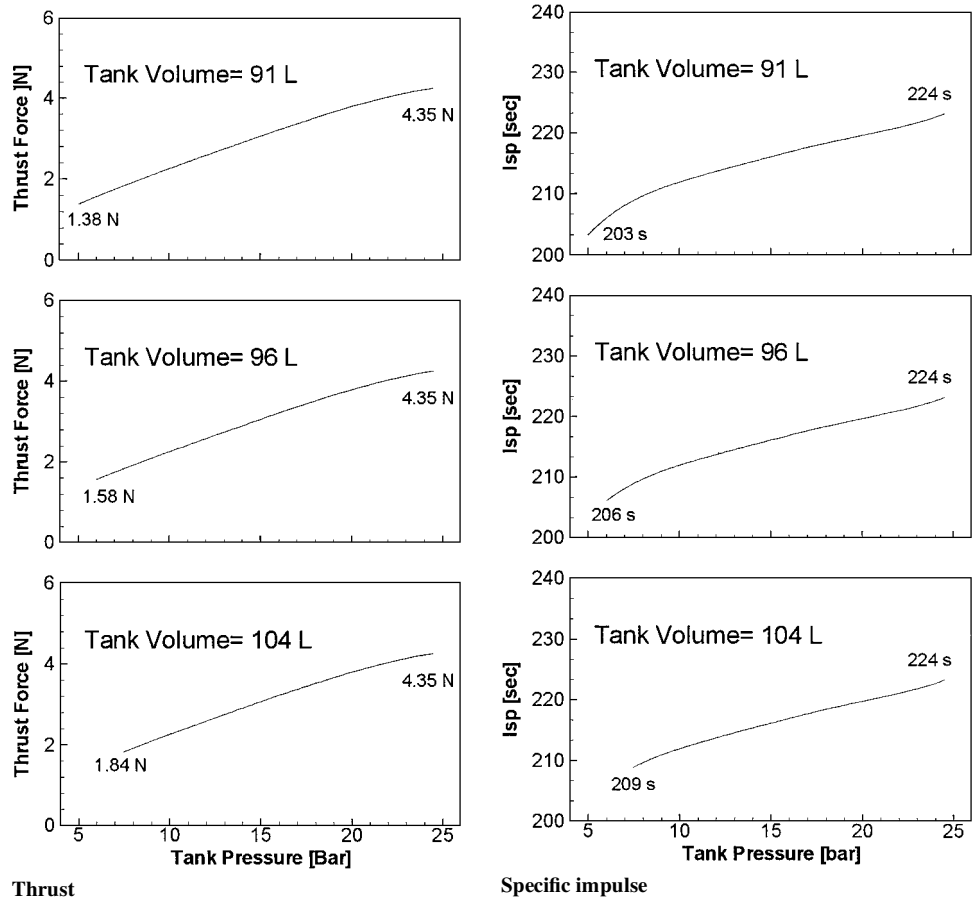

Thrust **Specific impulse**

Fig. 4 Entire blowdown pressure range for three different tanks; predicted.

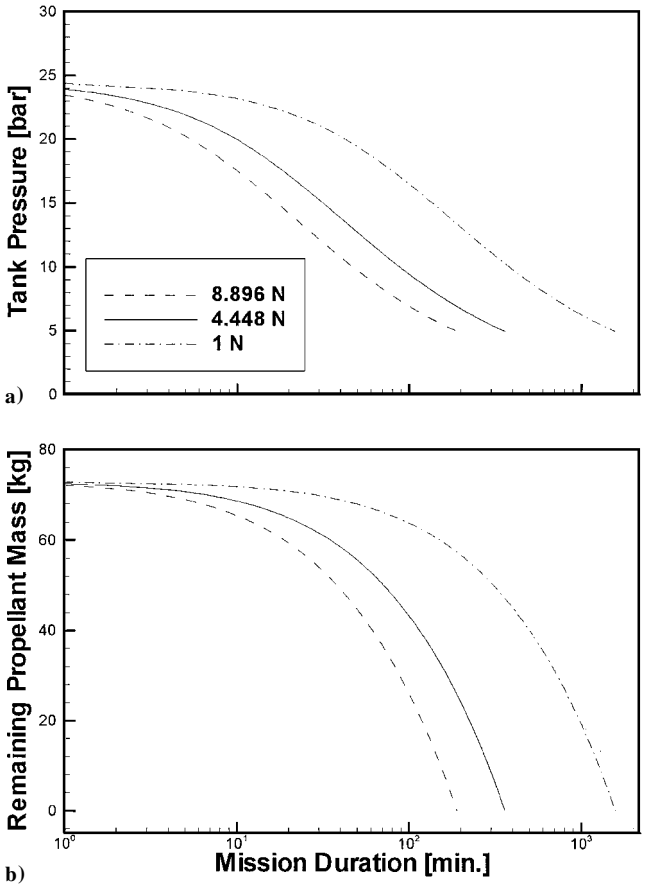

Fig. 5 Various thrust force levels, blowdown histories of a) tank pressure and b) remaining propellant mass along the mission duration.

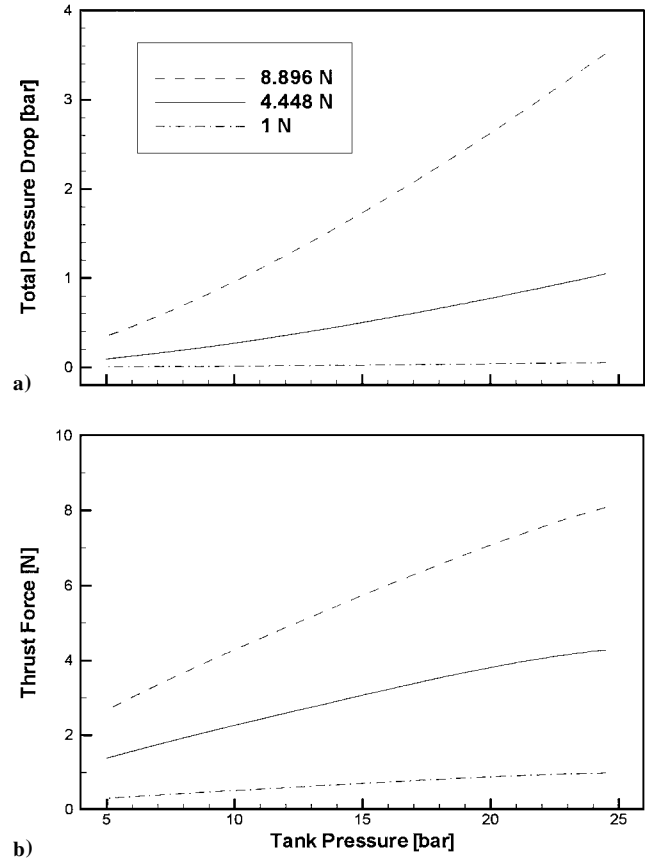

Fig. 6 Entire blowdown range for 1-, 4.448-, and 8.896-N thrusters: a) total pressure loss and b) thrust force.

For different missions, a larger tank potentially has the capability of carrying more propellants for meeting a wider scope of mission requirements. Nevertheless, because the propellant tanks usually occupy most of the propulsion system's volume, the space limitation, allowable center-of-mass offset of a satellite, and maintenance must be also taken into account to accomplish the tank selection and the location arrangement.

Successively, the mass flow rate effect on the propulsive performance was conducted. Three different values of mass flow rate [corresponding to 1-, 4.448-, and 8.896-N hydrazine thrusters] were examined. These kinds of thrusters have been commonly utilized in the propulsion system of low-Earth-orbit satellites. Figure 5 shows blowdown histories of the tank pressure and the remaining propellant mass along the mission duration at various thrust force levels. The remaining mass and tank pressure profiles stay relatively constant in the initial stage for all three cases. Because a larger propellant mass flow rate is required to sustain a continuous firing operation of thrusters with a higher thrust value, the hydrazine remaining mass and tank pressure curves for the 8.896-N case reduce substantially faster in comparison with those of the 1-N case. This observation suggests that the operation lifetime of using 8.896-N thrusters can be much shorter than that of using 1-N thrusters. The predicted time span values for the thrust force of 1, 4.448, and 8.896 N are 1580, 362, and 190 min throughout the lifetime of propellant usage. As shown in Fig. 6, the total line pressure loss and thrust were also computed over the entire blowdown pressure range for three examples. The total line pressure loss/thrust force at the maximum effective operating pressure (MEOP) of 24.5 bar are 3.51 bar/8.05 N, 1.05 bar/4.27 N, and 0.06 bar/0.98 N for the thrust level of 8.896 N, 4.448 N, and 1 N, respectively. Because of its high propellant mass flow rate through the hydrazine supply line, the total line pressure loss for the case of 8.896-N thruster is 14.3% of MEOP at BOL. This considerable pressure loss leads to a substantial decrease of the upstream pressure at the thrust inlet and in turn deteriorates the thrust output. For this calculation, the estimated thrust value at BOL is about 8.05 N, which is only 90% of the design thrust for a 8.896-N thruster. In practice, the requirement of maximum acceleration for a satellite orbit maneuver can establish criteria of thruster sizing for a specific mission envelope. The qualified capability of operating lifetime should be also considered in thruster selections.

The influence of various design features on the time-dependent transport behavior of the satellite hydrazine propulsion system is also studied using an MOC-based computer code. In simulations, all pipelines from the propellant tank to thruster valves were initially primed with hydrazine at 24.5 bar. Three cases of valve operations are investigated in this study: 1) instantaneous closing of the latching isolation valve, 2) instantaneous closing of four thruster valves, and 3) pulse train with a series of iterative open–close operations for thruster valves. To evaluate the fluid-hammer effect for the worst situations, all thruster valves are considered to be opened and closed simultaneously.

Before the closure of the latching valve, the latching valve and thruster valves are at the open position with a stable propellant flow through all pipelines. The latching isolation valve is then suddenly closed at $t = 0^+$ s. Figure 7a shows the transient pressure responses at the inlet of the latching isolation valve for various thrust-force levels. Caused by the abrupt closure of the latching isolation valve, the pressure immediately builds up to its peak and evolves fluctuant waves due to the outcome of the fluid hammer. The pressure responses act with a similar damping behavior for the other three thrust values with a nearly same decay time constant (defined as the time period of the amplitude ratio reducing from 1 to $1/e$) of 13.6 s^{-1}. Due to the surge-tank and friction effects, all pressure waves are damped out rapidly. These profiles converge toward their initial pressure of 24.5 bar within approximately 0.34 s. The maximum values of the predicted pressure rise for 1-, 4.448-, and 8.896-N thrusters are 0.94, 4.18, and 8.34 bar, respectively. Larger amplitudes of pressure oscillations are observed for the situation of

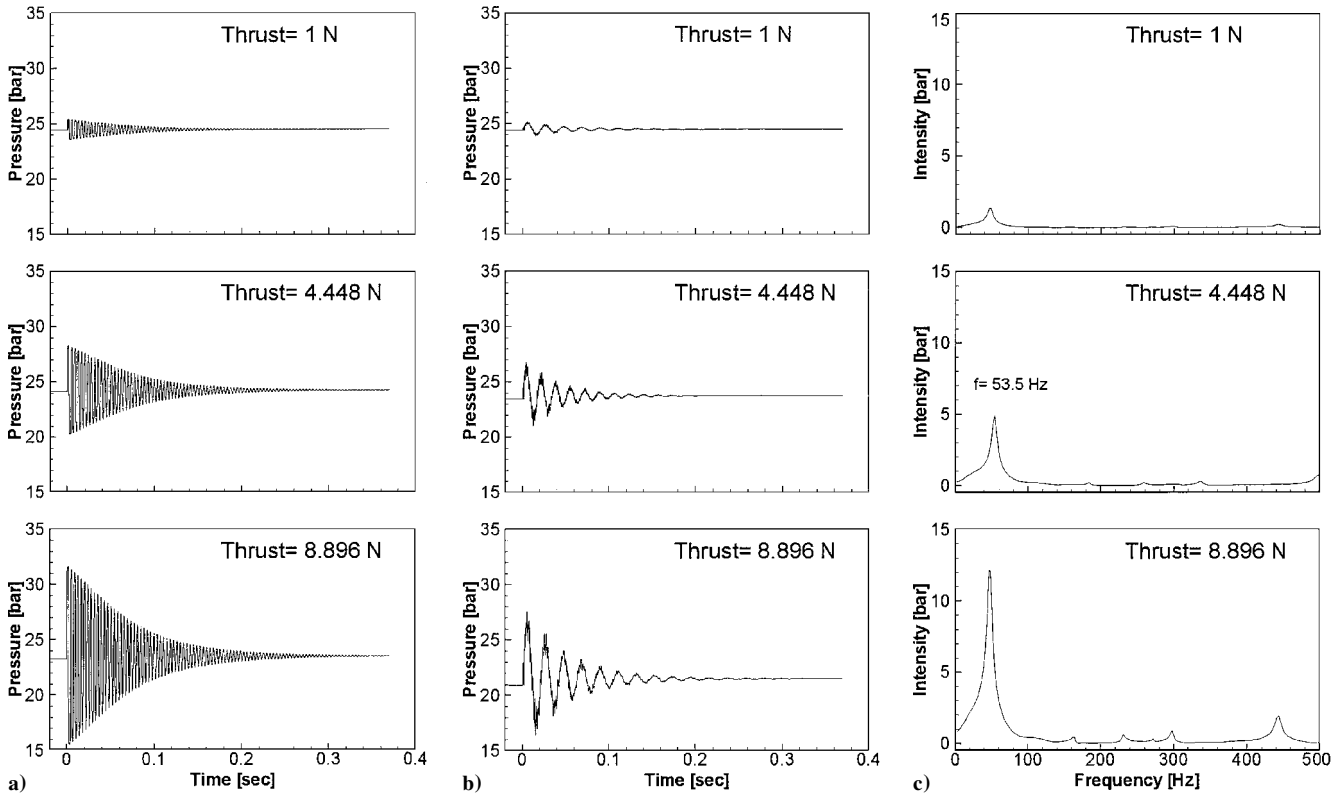

Fig. 7 Transient pressure at a) latching isolation valve inlet and b) thruster valve inlet for different thrust force levels, and c) Fourier spectral analysis of pressure waves at thruster valve inlet.

higher thrusts. The pressure rise tends to be linearly proportional to the thrust level. This trend shows that the predictions are consistent with the theoretical expectation. A high-pressure or fluid-hammer surge is formed in a flow system when a column of moving fluid is suddenly stopped. The flow kinetic energy is instantly converted into elastic energy, which compressed the liquid and expands the tube wall. The higher flow rate (or kinetic energy) would result in a higher surge in the lines. The pressure rise can be attributed to that a higher thrust force would entail a larger propellant flow rate through the pipeline and in turn lead to a greater pressure increase.

Because it is only a minor difference for pipeline lengths from the common junction (in the downstream of the latching isolation valve) to the four thrusters, the inlet pressure responses are almost identical for the four thrusters in the propulsion module. Figure 7b shows the pressure histories at one of thruster valve inlets for three cases. The thruster valves were closed instantaneously and simultaneously at $t = 0^+$ s. Similar to the results obtained in those cases of closing the latching isolation valve, the pressure profiles jump up to their first spike and oscillate with a larger value of the period for decay traveling sine waves. The pressure responses are then damped out quickly and approach 24.5 bar. Because of a relatively longer pipeline length for these calculations, the magnitudes of the pressure fluctuations are somewhat lower compared with those cases of closing the latching isolation valve.

In a hydrazine propulsion system, the isolation valve serves as a safety switch for protecting the system against failed open thruster valves or excessive leakage conditions. The operation sequences of shutting off propulsion functions start with the closure of the thruster valves and then to close the isolation valve. In practice, the closing of the isolation valve would not cause the fluid-hammer pressure surges in normal operations. Additionally, the Fourier spectral analysis for simulating the sudden closure of the isolation valve during contingency operations reveals that the first-mode frequency is about 263 Hz for the thrust force of 4.448 N, which is much higher than the design resonant frequency of fuel lines. Therefore, only the characteristics of the transient pressure waves at the thruster valve inlet are further probed in this study. When the pressure fluctuations are transformed from the time domain (as shown in Fig. 7b) to the frequency domain, various modes of pressure waves can be determined using the Fourier spectral analysis. In the structure analysis of the propulsion system, the resonant frequencies of the thruster assembly and fuel lines are typically required to exceed 130 and 75 Hz, respectively, to assure structure integrity. Figure 7c shows the results of the Fourier spectral analysis for the pressure fluctuations at the thruster valve inlet. For three cases, Fig. 7c clearly indicates a number of wave modes with the highest peak of intensity at the frequency of 53.5 Hz. This corresponding peak spectral intensity is found to increase with the thrust force level. In addition, the first-mode frequency of 53.5 Hz is substantially lower than the design resonant frequencies of the thruster assembly and fuel lines stated in the hydrazine propulsion system design specifications. It can be then ensured that the induced excitation from the fluid-hammer pressure oscillations will not resonantly couple with the earlier mentioned propulsion structure elements.

For most propulsion systems with medium to high thrust values, orifices are often installed in the pipeline to mitigate excessive pressure oscillations. In the ROCSAT-1 design, an orifice is located between the filter and the latching isolation valve as shown in Fig. 1. The size of the orifice is 0.099 cm (0.039 in.) in diameter. Figure 8 shows the transient pressure at the latching isolation valve inlet and thruster valve inlet for the situations without and with an orifice installed. Before the sudden closure of the latching isolation valve or thruster valves, four 4.448-N thrusters were firing simultaneously at the tank pressure of 24.5 bar for all cases. The maximum pressure achieved at the latching isolation valve inlet and thruster valve inlet is 28.51 and 27.52 bar, respectively, for the case where no line orifice is installed. As observed in Fig. 8a, the use of an orifice rapidly damps out the pressure oscillations within 0.25 s compared with the case without using an orifice. This fast damping phenomenon of the pulsating pressure waves results from the strong damping effect influenced by the orifice. Similar results are exhibited in Fig. 8b. The pressure fluctuations at the thruster valve inlet dissipated in a short time for the case of placing an orifice in the line. Simulations

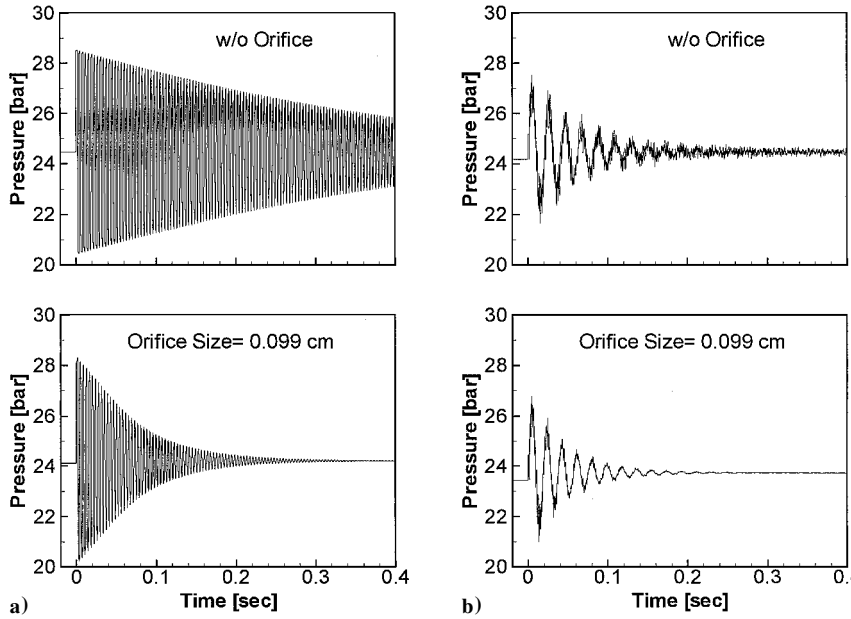

Fig. 8 Transient pressure at a) latching isolation valve inlet and b) thruster valve inlet for conditions without and with orifice installed.

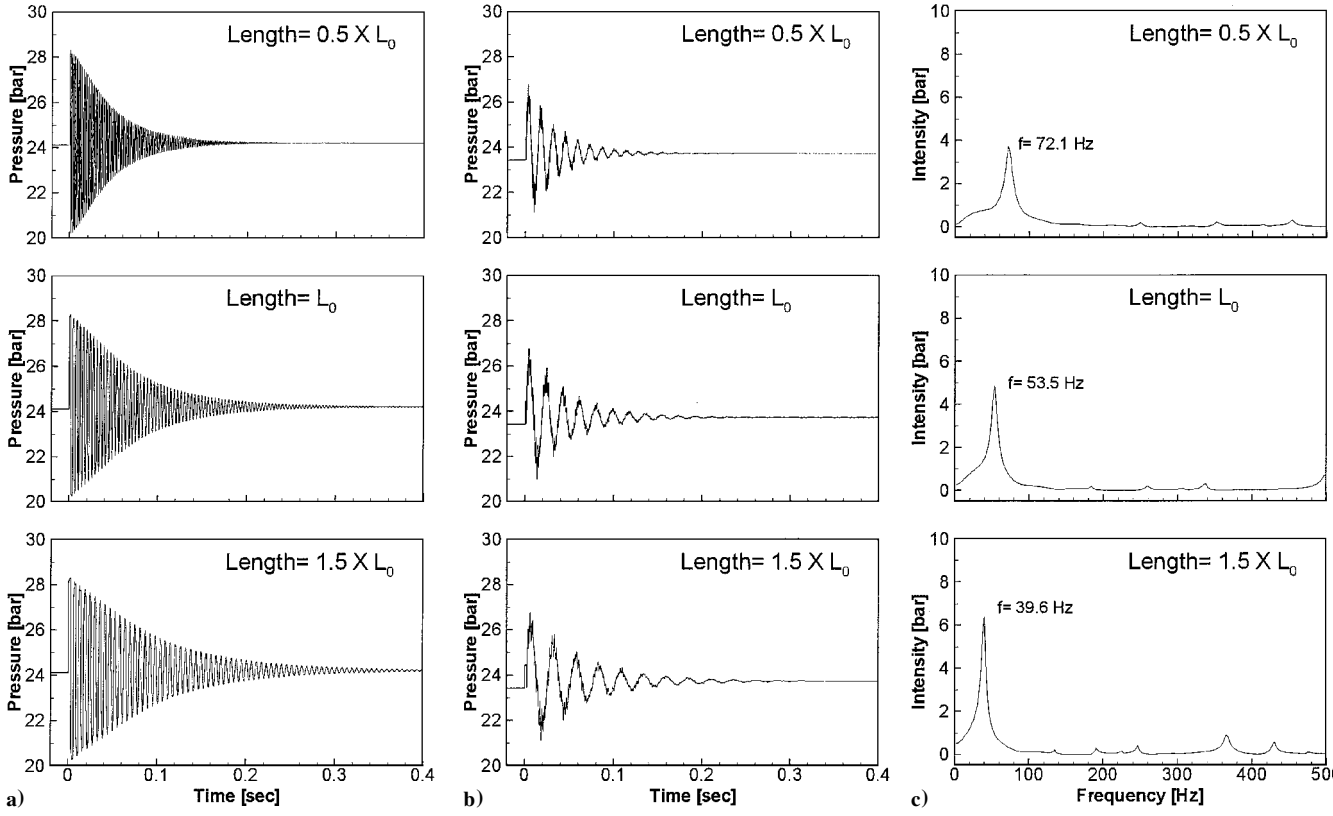

Fig. 9 Transient pressure at a) latching isolation valve inlet and b) thruster valve inlet for different pipeline lengths, and c) Fourier spectral analysis of pressure waves at thruster valve inlet.

clearly indicate that the potential risk of damaging propulsion components by the fluid-hammer-induced pressure oscillations can be minimized using some appropriate orifices.

The effect of geometrical dimension on the time-dependent flow behavior was also studied. Three different pipeline lengths ($0.5L_0$, L_0, and $1.5L_0$) were considered in simulations, where L_0 is the total pipeline length of the ROCSAT-1 propulsion system. For different total pipeline lengths, Fig. 9 shows the transient pressure histories at the latching isolation valve inlet and thruster valve inlet, as well as the Fourier spectral plots of pressure waves at the thruster valve inlet. For all cases, the maximum pressure raises attained at the latching isolation valve inlet and thruster valve inlet are nearly same, with the magnitude of 4.1 and 3.3 bar, indicating that the pressure raise is not sensitive to the change of pipeline length as the thrust force is determined. Based on the theoretical model, the peak pressure surge is equal to the product of fluid density, acoustic speed, and flow velocity, which reveals that the maximum pressure surges are not affected by line length. Simulations clearly demonstrate that the calculated results are in agreement with the theoretical analysis. Because the frequency of the pressure response is equal to

the acoustic speed divided by the traveling distance of the wave, a higher frequency of the pressure waves occurs for a shorter pipeline length. Then it can be expected that, within a fixed time interval, the iterative number for the pressure wave propagating back and forth in a shorter pipeline is greater than that of a longer pipeline. This flow behavior can result in the stronger friction and surge-tank effects and successively lead to a more rapid decay rate of the damped pressure oscillation in a shorter pipeline. Therefore, the decay time constants of the damped pressure fluctuation at the latching isolation valve inlet are 23.1 s^{-1} for $0.5L_0$, 13.8 s^{-1} for L_0, and 10.4 s^{-1} for $1.5L_0$, respectively. The pressure response in the time domain at the thruster valve inlet was further converted into the spectral intensity in the frequency domain through the Fourier spectrum analysis. As the total pipeline length increases, larger flow inertia mass is involved in a fluid vibratory system, which tends to lower the first-mode frequency and substantially augment its spectral intensity for a longer pipeline. It is also observed that the intensities at higher-mode frequencies for all cases are insignificant.

A series of thruster valve opening–closing operations, that is, pulse train operations, is a very common practice for the purpose of satellite attitude control. Figure 10 shows the transient responses of the pressure and mass flow rate at the thruster valve inlet (with the thrust force of 4.448 N) for pulse train operations. In the present study, there are four testing conditions based on the different setting of valve operations. The corresponding time periods for each valve open/closed are 30/220 ms, 50/200 ms, 80/170 ms, and 100/150 ms for simulating a typical pulse mode thruster firing sequence during a 250-ms attitude control cycle. From the predictions for all four cases, the damped pressure oscillation tends to reach its steady state; however, the follow-up valve operation stops this converging trend and initiates another bundle of damped pressure oscillations. It is observed that the peak values of the time-dependent pressure profiles are 28.6, 28.1, 27.6, and 27.6 bar for the valve opening time of 30, 50, 80, and 100 ms, respectively. Because of the closed coupling of the pressure with the mass flow rate, the fluid-hammer-induced pressure oscillation causes the fluctuation behavior of the propellant mass flow rate. In the very beginning of the valve opening time interval, the maximum magnitude of the mass flow variation could be up to ±33% during the steep buildup, while the corresponding highest difference for pressure fluctuations is about ±17%. For the conditions of 30- and 80-ms valve opening time, the mass flow rate variations are about ±5 and ±0.7% at the end of the valve-opening time interval. From the design point of view, smaller valve-opening time interval can reduce the impulse bit (defined as the product of thrust by firing duration) that would generally acquire a better accuracy of thruster-based attitude control and then enhance the pointing performance of the satellite. On the other hand, the propellant mass flow rate fluctuation may also lead to a considerable

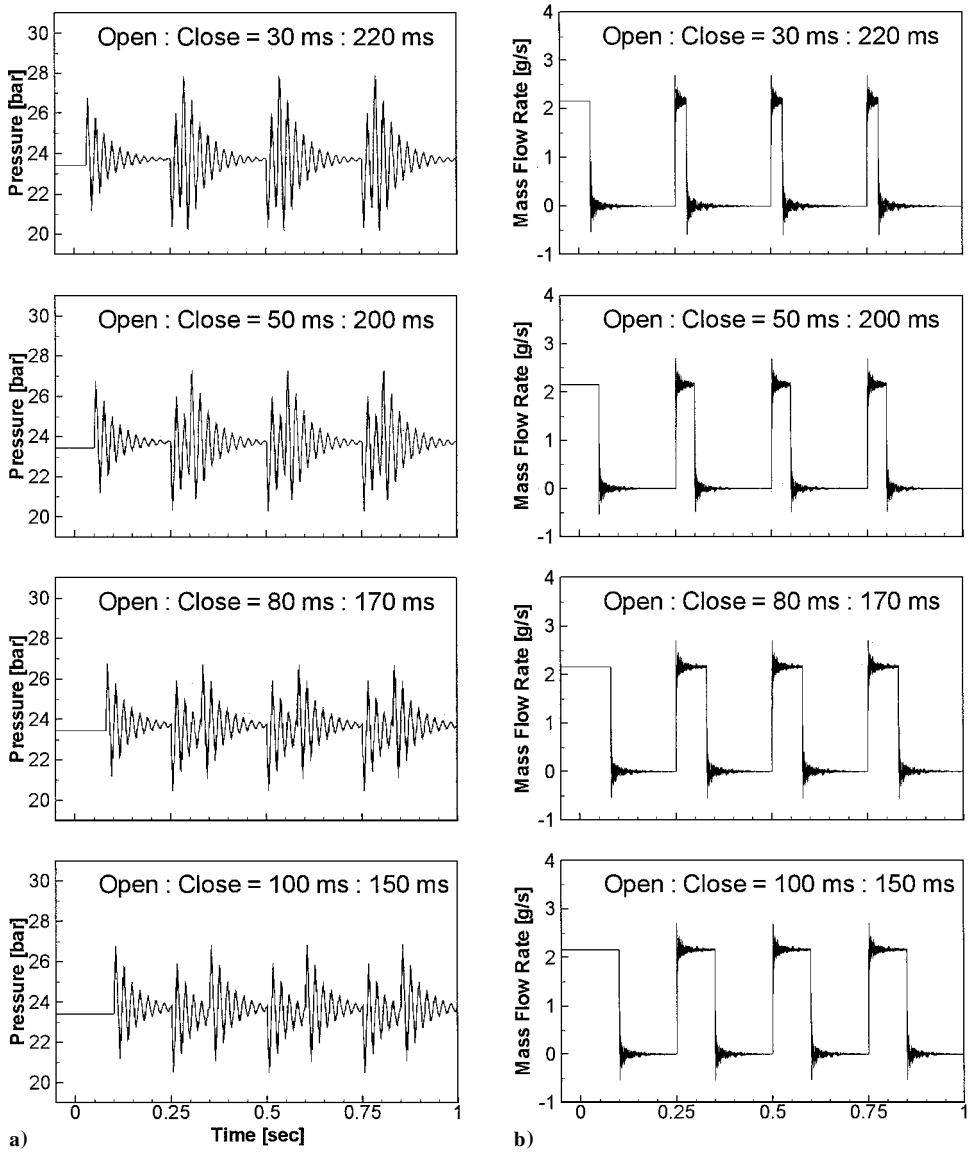

Fig. 10 Transient histories of a) pressure and b) mass flow rate at thruster valve inlet for various pulse train operations.

thrust variation and lower specific impulse. Both effects need to be considered for achieving an optimum control. In this analysis, it is found that the setting of an 80-ms opening time interval can maintain a relatively stable propellant mass flow rate at the pulse-mode operations for rendering a reasonable propulsive performance.

Conclusions

The configuration of a satellite hydrazine propulsion system has been studied using numerical analysis. Some key parameters for driving the flow behavior of blowdown and fluid-hammer characteristics have been examined in detail. The results obtained from the simulations are concluded as follows.

1) Three different tanks with the volume of 91, 96, and 104 liters were considered to analyze the tank sizing effect. The performance using the 104-liter tank shows an enhancement of 33% thrust force increase and 3% specific impulse improvement over the system employing the 91-liter small tank.

2) Three kinds of commonly utilized thrusters in the satellite propulsion system were chosen to study the influences for the thrust force level effects. The predicted time span value of using 8.896-N thrusters will be only 12% of that using 1-N thrusters, and only 90% of the design thrust can be obtained due to the large pressure loss in the pipeline.

3) For different thrust force levels of the transient fluid analysis, the pressure rise tends to be linearly proportional to the thrust level, and all pressure waves will be damped out rapidly, as a result of the friction and surge-tank effects. The results indicate that the resonant frequencies are around 53.5 Hz, which is insensitive to the thrust force variations. All of these values are lower than the design frequencies of thruster assembly and fuel lines that are given in the propulsion specifications.

4) In present work, the simulation shows that the potential risk of damaging propulsion components by the fluid-hammer-induced pressure oscillations can be minimized using appropriate orifices, and the pressure oscillation will be damped out within 0.25 s.

5) Simulations for different pipeline lengths were performed. The data illustrate a rapid decay rate can be obtained due to the stronger friction and surge-tank effects for shorter pipeline condition. As the total pipeline length increases, larger flow inertia will be involved in the fluid vibratory system, which tends to lower the resonant frequencies and augment the spectral intensity.

6) Observation of the pulse-train simulations shows that a shorter opening period in 0.25-s control cycle will result in a higher peak value of the time-dependent pressure profiles and cause the mass flow rate fluctuation leading to a considerable thrust variation and lower specific impulse. From this analysis, the setting of 80-ms opening time can maintain a relatively stable propellant mass flow rate at the pulse-mode operations.

Acknowledgment

This work represents part of the results obtained under Contract NSC90-2212-E-212-029, sponsored by the National Science Council, Taiwan, Republic of China.

References

[1]Wertz, J. R., and Larson, W. J., *Space Mission Analysis and Design*, 3rd printing, Kluwer Academic, Dordrecht, The Netherland, 1991, Chap. 17, pp. 579–603.

[2]Sutton, G. P., *Rocket Propulsion Elements*, 6th ed., Wiley, New York, 1992, Chap. 10, pp. 281–364.

[3]Huzel, D. K., and Huang, D. H., "Design of Liquid Propellant Space Engines," *Modern Engineering for Design of Liquid Propellant Rocket Engines*, Vol. 174, Progress in Astronautics and Aeronautics, AIAA, Washington, DC, 1992, Chap. 11, pp. 373–388.

[4]Hasan, D., Adler, S., Oren, A., and Miller, N., "Propulsion Systems for Small Satellites," *Space Technology*, Vol. 15, No. 6, 1995, pp. 375–381.

[5]Bellerby, J. M., "Hydrazine as a Propellant for Space Systems," Chemical System Group, Cranfield Inst. of Technology, Royal Military College of Science, Shrivenham, England, U.K.

[6]Blazer, D. L., Brill, Y. C., Scott, W. R., and Sing, P. Y., "The Monopropellant Hydrazine Reaction Control System for the RCA SATCOM Satellite," *AIAA/SEA 12th Propulsion Conference*, AIAA Paper 76-631, July 1976.

[7]Agrawal, B. N., McClelland, R. S., and Song, G., "Attitude Control of Flexible Spacecraft Using Pulse-Width Pulse-Frequency Modulated Thrusters," *Space Technology*, Vol. 17, No. 1, 1997, pp. 15–34.

[8]Molinsky, J., "Water Hammer Test of the SeaStar Hydrazine Propulsion System," *33rd AIAA/ASME/SEA/ASEE Joint Propulsion Conference*, AIAA Paper 97-3226, Seattle, WA, July 1997.

[9]Sansevero, V. J., Jr., and Garfinkel, H., "Flight Performance of the Hydrazine Reaction Control Subsystem for the Communication Technology Satellite," *AIAA/SEA 12th Propulsion Conference*, AIAA Paper 76-630, July 1976.

[10]Zielke, W., "Frequency-Dependent Friction in Transient Pipe Flow," *Journal of Basic Engineering*, Ser. D, Vol. 90, No. 1, 1968, pp. 109–115.

[11]Trikha, A. K., "An Efficient Method for Simulating Frequency-Dependent Friction in Transient Liquid Flow," *Journal of Fluids Engineering*, Vol. 97, No. 1, 1975, pp. 97–105.

[12]Schohl, G. A., "Improved Approximate Method for Simulating Frequency-Dependent Friction in Transient Laminar Flow," *Journal of Fluids Engineering*, Vol. 115, No. 3, 1993, pp. 420–424.

[13]"Request for Proposal for the ROCSAT-1 Spacecraft," National Space Program Office, Document NSPO-RFP83-001, Hsinchu, Taiwan, Republic of China, Dec. 1993.

[14]Steeter, V. L., and Wylie, E. B., *Fluid Transients in System*, Prentice–Hall, Upper Saddle River, NJ, 1993, Chaps. 2, 3, pp. 20–79.

[15]Hsieh, W. H., Lin, C. Y., and Yang, A. S., "Blowdown and Waterhammer Behavior of Monopropellant Feed Systems for Satellite Attitude and Reaction Control," *33rd AIAA/ASME/SEA/ASEE Joint Propulsion Conference*, AIAA Paper 97-3224, Seattle, WA, July 1997.

[16]Simpson, A. R., "Large Water Hammer Pressure Due to Column Separation in Sloping Pipes," Ph.D. Dissertation, Univ. of Michigan, Dept. of Mechanical Engineering, Ann Arbor, MI, May 1986.